Build. Sci. Vol. 4, pp. 119–132. Pergamon Press 1969. Printed in Great Britain

SfB	Ab 4
UDC	624.073

An Experimental Study of the Ultimate Load Behaviour of Composite Steel–Concrete Bridge Deck Structures

V. M. REDDY* Ph.D., B.E., M.Sc., A.M.I.C.E.
A. W. HENDRY† Ph.D., D.Sc., M.I.C.E., M.I.Struct.E.

This article describes tests on eight model bridge decks of composite steel beam–concrete slab construction. The aim of the work reported was to provide experimental data for the development of a theoretical method for the prediction of the ultimate strength of bridge decks of this type based on yield line analysis. Simply supported bridge decks having three and four longitudinals were tested under a variety of loading conditions.

INTRODUCTION

COMPOSITE construction, using structural steel sections and cast *in situ* slabs, has long been used in bridges. However, it was only recently that the British Standards Institution has published Code of Practice, C.P.117 (1967), part 2 relating to this type of structure[1].

The analysis of a composite beam bridge is complicated owing to the presence of T-beam action. The predominating failure of such T-beams observed in tests[2–4] being tension failure of steel, it is reasonable to assume that the moment of resistance is sensibly constant at failure thus permitting the application of yield line methods for calculation of failure loads. Though idealised plastic theories for slab and T-beam action combined are open to criticism, nevertheless such theories are likely to be conservative owing to the effects of membrane action and strain-hardening of steel[5].

Because of the complexity of a composite beam bridge, the applicability of any analysis can be determined only by comparing the behaviour of actual structures with that predicted by analysis. With this in mind, laboratory tests have been carried out on eight model composite beam bridges. The purpose of these tests was to determine the ultimate capacity of the bridges and their manner of failure under different loading conditions for comparison with possible theoretical estimates of ultimate strength and to obtain further information on the behaviour of the composite beam and slab elements which constitute the structure. The purpose of this report is to give an account of these experiments but comparisons are given with theoretical results, the basis of which is discussed in detail elsewhere[4, 12].

DESCRIPTION OF MODELS AND TESTING ARRANGEMENT

The tests were divided into two groups referred to as A-series and B-series. The specimens of A-series had three longitudinals with a span of 72 in. and a slab width of 36 in. In the specimens of B-series, the span was kept the same but there were four longitudinals with a slab width of 48 in. The variable in each group of the tests was the type of loading which consisted of concentrated loads only. The layout and loading, modes of collapse, the crack patterns after failure and the theoretical yield patterns for all the models tested are given in various diagrams which may be located from Table 1.

Steel joists were connected to the slab by mechanical shear connectors, which were designed according to the procedure given in C.P.117, part 1[6]. A typical load–slip curve is shown in figure 3. It was assumed that complete composite action between the beams and the slab existed up to failure. The spacing of beams was chosen in order to keep the effect of shear lag[7] to a minimum so that nearly the entire width of slab available would be effective in acting as a compression flange of the beam. The design details of models are given in Table 2 and the typical sections in figure 4. The properties of the steel used in the beams and in the reinforcement of the slab are given in Tables 3 and 4 respectively. The properties of concrete control cubes are given in

* Head of Structural Engineering Section, Regional Engineering College, Warangal-4, A.P. India.
† Department of Civil Engineering and Building Science, University of Edinburgh, Edinburgh.

Table 1

Model	Lay-out and loading and modes of collapse	Load spacing ratio (see figures 1, 2 and 3)	Crack patterns after failure (figure no.)
A I and A II	Fig. 1a	0	6
A III	Fig. 1b	1/6	9
A IV	Fig. 1a	5/36	10
B I	Fig. 2b with additional loads at the points 3, 4, 7 and 8	1/6	11
B II	Fig. 2b	5/36	15
B III	Fig. 2a	5/36	16
B IV	Fig. 2a with loads at points 3 and 4 omitted	5/36	17

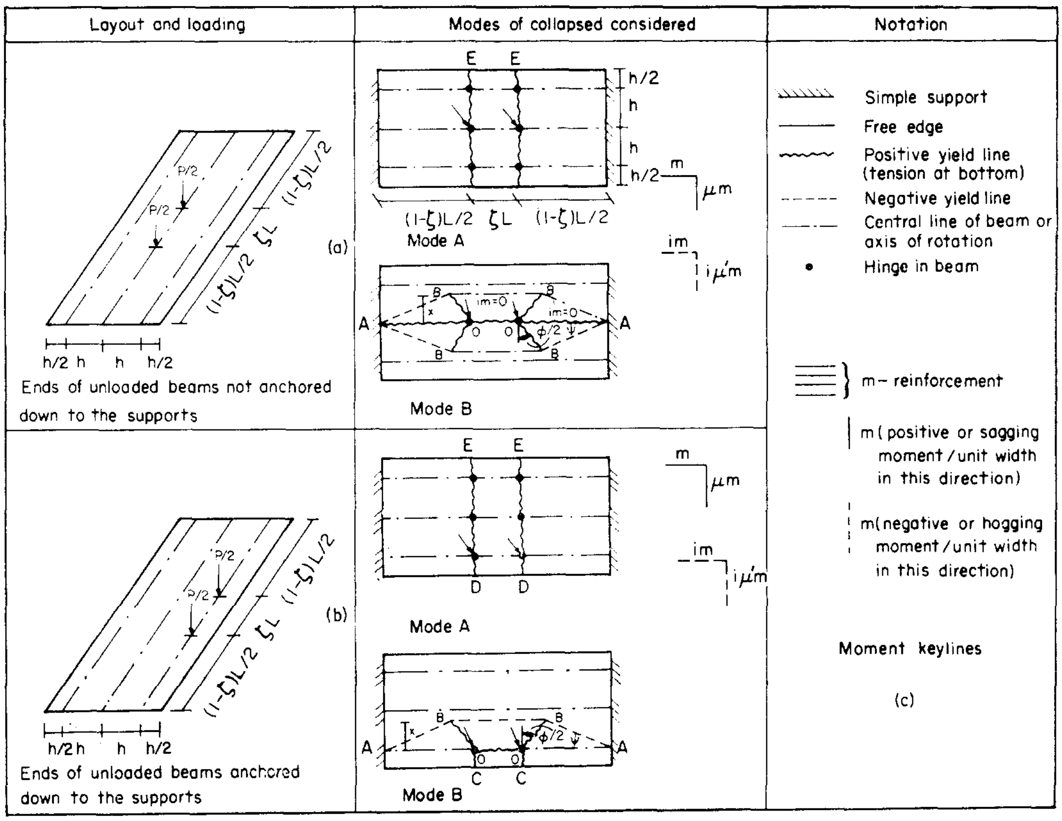

Fig. 1. Three longitudinal bridge decks.

Table 5. Preceding the test on each model, control tests were conducted to determine the properties of single elements, namely (i) composite beam (ii) slab strips in transverse and longitudinal directions.

A loading frame specially constructed for the investigation with Model A I ready for test is shown in figure 5. The strains were measured across the depth of the composite beams at mid span using $\frac{1}{2}$ in. gauge length electrical resistance gauges. The concrete surface strains were measured using a 2 in. gauge length Demec Gauge and also resistance gauges of 20 mm gauge length. The deflections at mid span were measured using dial gauges reading to 0·001 in. and 0·0001 in.

DISCUSSION OF TEST RESULTS

The applicability of yield-line theory to a composite steel–concrete structure depends mainly on the properties of the steel used. The strength of the concrete is secondary but it should not be so weak as to affect the load–slip characteristics of the shear connectors[8] which may result in splitting along the line of the connectors. This was observed in Model A IV (figure 10) which was cast in concrete of lower strength (Table 5).

The steel used in beams of models of A-series, as revealed by tensile tests (Table 3), developed strain-hardening to a considerable extent. Tests in-

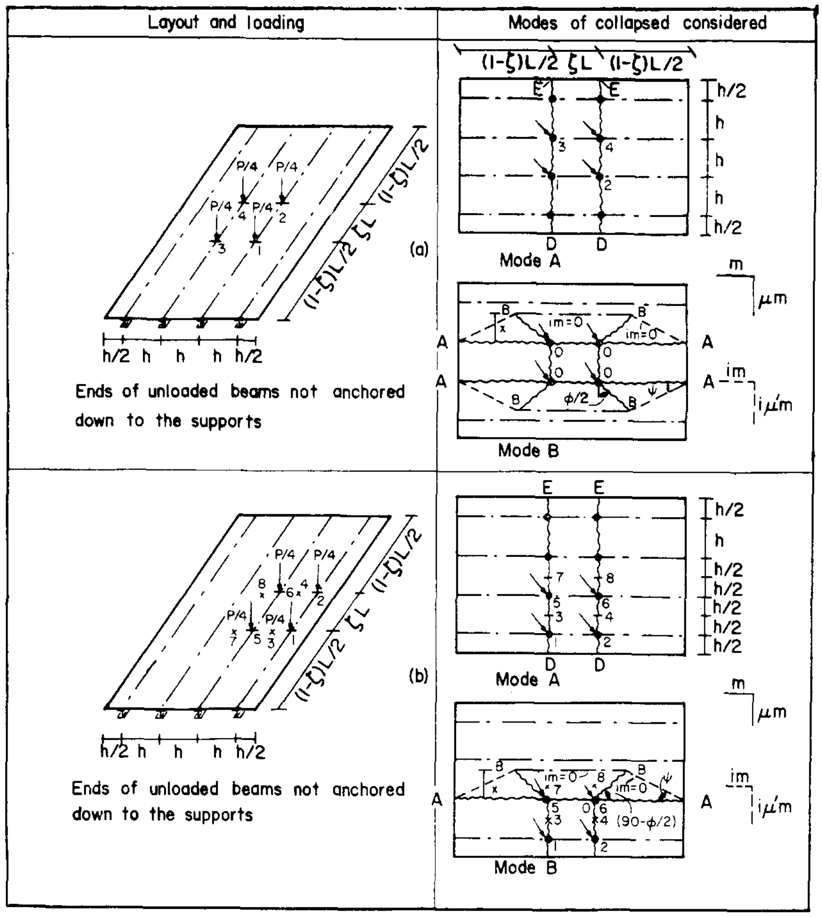

Fig. 2. Four longitudinal bridge decks.

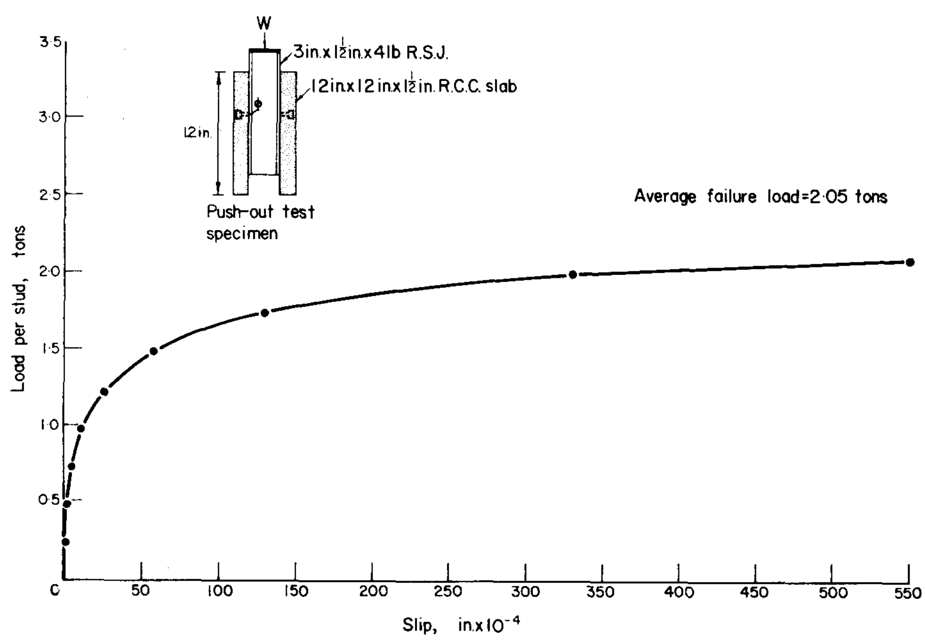

Fig. 3. Load–slip curve from a typical push-out test.

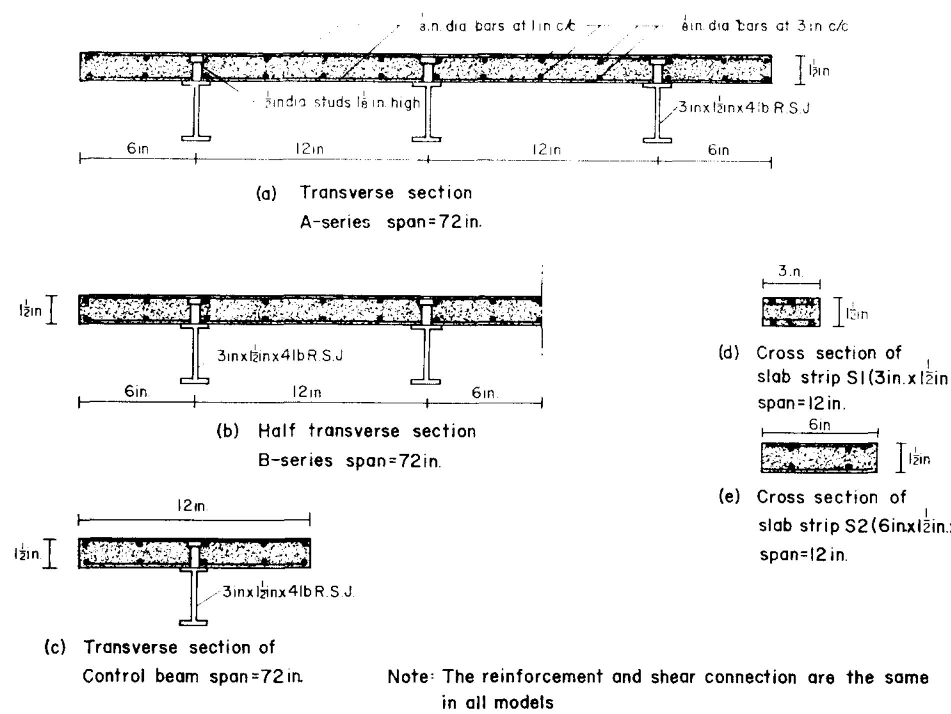

Fig. 4. Sections of models.

Table 2. Design details for all model bridges

	span, in.		72
	spacing of beams, in.		12
Steel joists	size, in.		$3 \times 1\frac{1}{2}$
	weight, lb/ft.		4
	cross sectional area, in^2		1·18
	Modulus of section, in^3		1·11
Shear connectors	Type		Headed stud
	Diameter, in.		$\frac{1}{2}$
	Height, in.		$1\frac{1}{8}$
	spacing, in.		2
	Total number in span		36
	Depth of slab, in.		$1\frac{1}{2}$
	Slab reinforcement		All bars $\frac{1}{8}$ in. diameter
Transverse	Bottom	spacing, in.	1
		per cent	0·94
	Top	spacing, in.	1
		per cent	0·94
Longitudinal	Bottom	spacing, in.	3
		per cent	0·34
	Top	spacing, in.	3
		per cent	0·34

dicate that strain-hardening has a beneficial effect on the ultimate capacity of a structure, though it complicates the analysis.

The pattern of yield lines that may develop in a beam and slab system largely depends on:

(i) Ratio of ultimate moments in longitudinal and transverse directions,

(ii) Spacing of beams,

(iii) Support conditions, and

(iv) Type of loading.

In the present tests, the only variable in each group of tests was the type of loading and therefore the present paper is concerned with the behaviour of the test specimens under different loading conditions.

DEGREE OF COMPOSITE ACTION

The ultimate capacity of one shear connector found from a push-out test was 2·05 tons against the maximum design force of 1·32 tons. The slip corresponding to this force was only 26×10^{-4} in. (figure 3). This is much less than the safe value[8] at which full interaction could be assumed without introducing any appreciable error in calculating the maximum moment.

The strains measured show that the strain-distribution is more or less linear across the depth of the composite section (figure 14) implying that any slip present at the interface can be ignored.

BEHAVIOUR OF CONTROL BEAMS AND SLAB STRIPS

The failure of all the control beams was by the formation of a compression crack across the width of the slab at the section of maximum moment[4].

Table 3. Properties of steel in beams

Series	Size of beam	No. of tests	Yield point f_y (lb/in²)	Per cent ultimate strength f_u (lb/in²)	Per cent strain at first yield e_y	Per cent strain at strain hardening e_s	E (lb/in²)	E_{sh} (lb/in²)	$s = E/E_{sh}$	$r = e_s/e_y$
A	3 in. × 1½ in. × 4 lb.	6	45,000	69,000	0·15	0·15	30×10^6	1×10^6	30	1
B	3 in. × 1½ in. × 4 lb.	6	35,000	63,000	0·118	1·53	$29{\cdot}5 \times 10^6$	$0{\cdot}473 \times 10^6$	62·5	13

E = Young's modulus
E_{sh} = strain hardening modulus

Table 4. Properties of ⅛ in. dia. reinforcing bars of slab obtained from tensile tests on 2 in. G.L. specimens

Series	No. of tests	Yield point (approx.) (lb/in²)	Ultimate strength (lb/in²)
A	3	63,000	71,000
B	3	65,900	95,700

The steel section was fully plastic in almost all the tests. The neutral axis moved upwards after the bottom flange of the beam yielded and was in the slab at maximum moment. The longitudinal reinforcement at the top of the slab yielded at maximum moment.

The tests gave the values of ultimate moments, which were generally higher than the theoretical ones, calculated on the assumption that concrete attains 2/3 cube strength or the value given by Hognestad's stress block[9] at maximum moment. The ultimate moment calculated on the basis of 4/9 cube strength (C.P.117 part 1, 1965) is conservative. The gap between theory and test was as high as 30 per cent in the beams of A-series and 20 per cent in B-series, even after an allowance was made for the effect of strain-hardening in the

Table 5. Properties of concrete obtained from tests on 4 in. and 6 in. cubes

(Concrete mix: Cement, fine sand and coarse sand were in the proportion 1:2:3 by weight. Water–cement ratio = 0·60 by weight)

Model	Age at test (days)	No. of tests on: 4 in. cube	No. of tests on: 6 in. cube	Average cube strength (lb/in²)
A I	40	3	3	5227
A II	47	3	3	5096
A III	54	3	3	6290
A IV	56	3	3	3280
B I	30	3	3	5130
B II	37	3	3	6270
B III	44	3	3	5600
B IV	44	3	3	5600

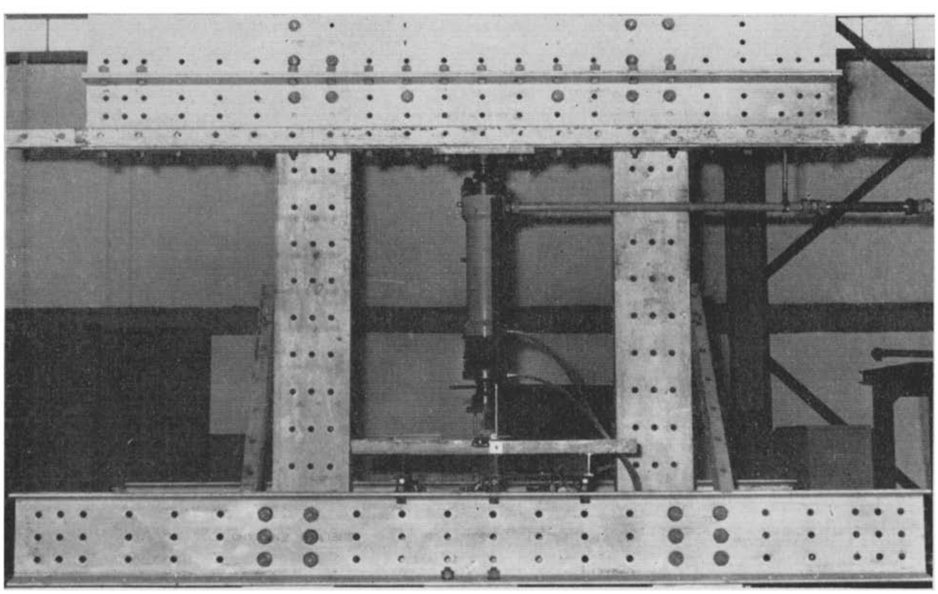

Fig. 5. View of loading frame with Model AI ready for test.

Table 6. Values of $\phi/2$, ψ and x for yield patterns (see figures 1 and 2)

Model	Equivalent slab method			Beam and slab method			Experimental (average)		
	$\phi/2$	ψ	x (in.)	$\phi/2$	ψ	x (in.)	$\phi/2$	ψ	x (in.)
A I and A II	51° 34′	38° 26′	14·3	56° 18′	38° 42′	12	57° 0′	34° 0′	12–15
A III	33° 42′	26° 42′	11·3	32° 0′	28° 6′	12	32° 30′	25° 0′	10–12
B I	59° 24′	56° 30′	12·8	61° 0′	55° 0′	12	50° 0′	48° 0′	12–18
B II	56° 12′	54° 24′	14·0	60° 6′	53° 30′	12	50° 0′	50° 0′	12–18
B III	56° 54′	53° 30′	13·7	60° 6′	53° 36′	12	51° 0′	50° 0′	12–14

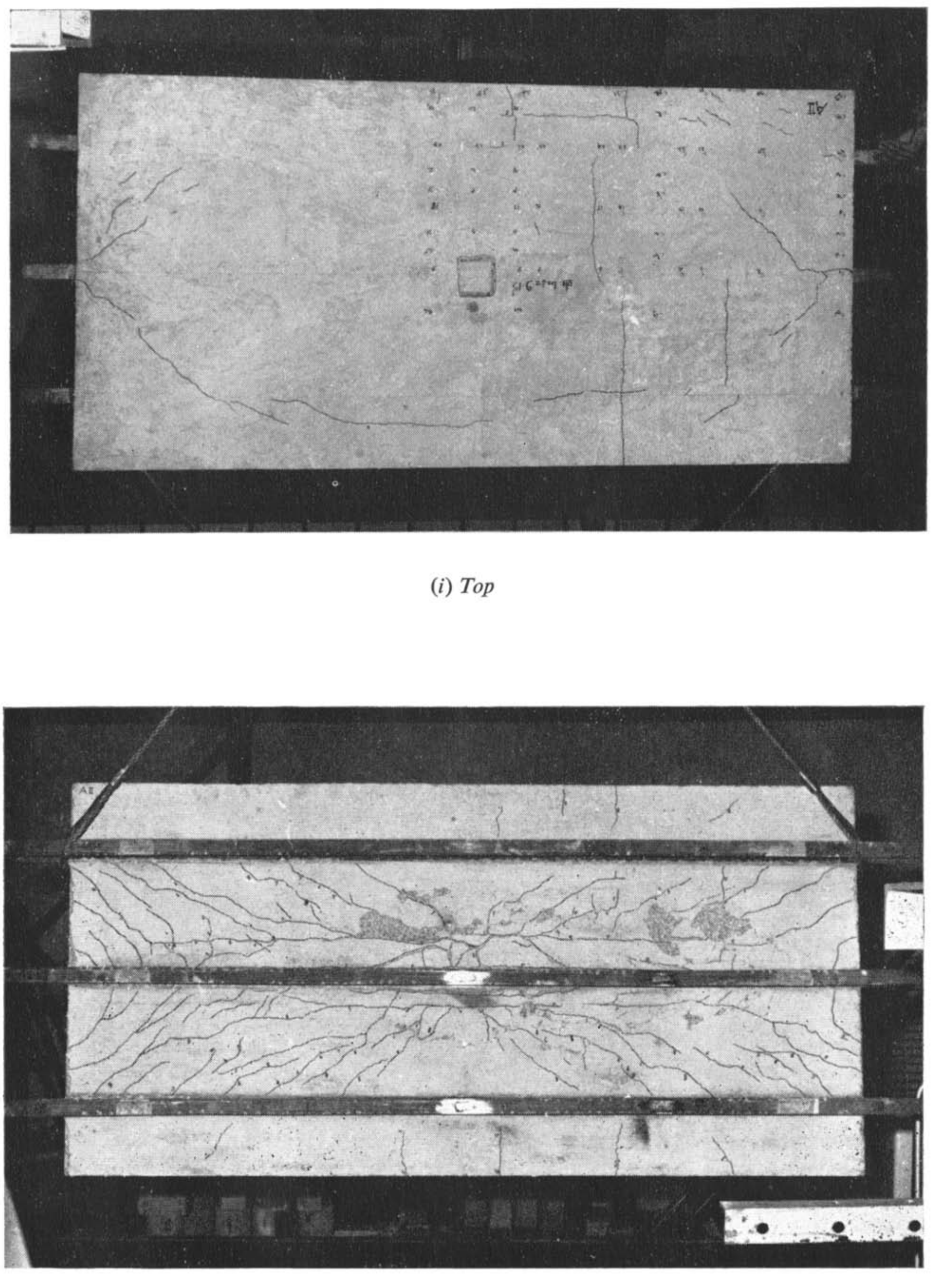

(*i*) *Top*

(*ii*) **Bottom**

Fig. 6. Crack pattern of Model AII after failure.

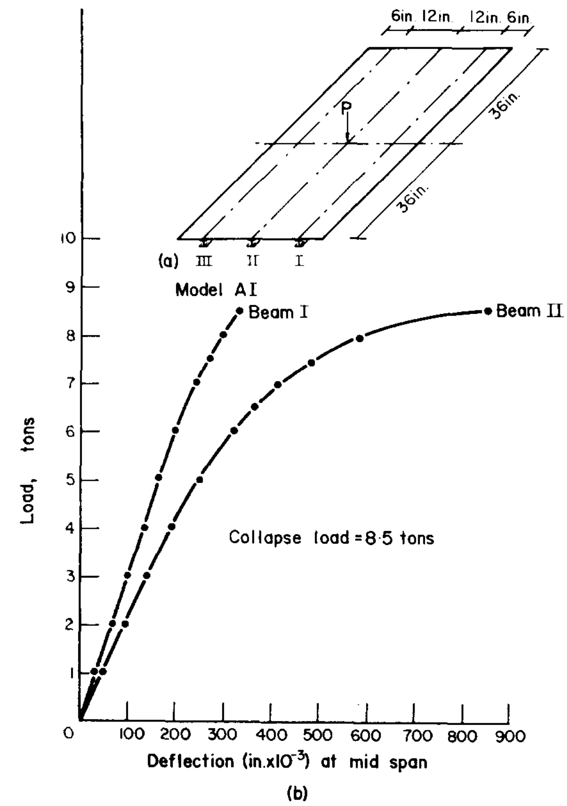

Fig. 7.

theory[4]. This was expected because of the limit put on the maximum value of concrete edge strain at maximum moment. The theoretical values of this strain[9] varied from 0·318 to 0·334 per cent for different strengths of concrete used against the experimental values which varied from 0·35 to 0·50 per cent. By permitting higher values of this strain observed in tests, this gap could be considerably reduced, but how far this is justified is in doubt because of many uncertainties inherent in the strain-hardening nature of steel and the strain-softening nature of concrete.

The ultimate moments of slab strips obtained from tests were in reasonable agreement with theoretical values which were on the safe side.

BEHAVIOUR OF BEAMS IN MODELS

The deflections and strains of beams in Models A I and B I, which are typical of other models, are shown in figures 7 and 8 and figures 12–14 respectively.

First yielding of the beams was characterised by an abrupt change in the slope of load–strain curves. Yielding occurred first in the loaded beam and was shortly followed by large deflections.

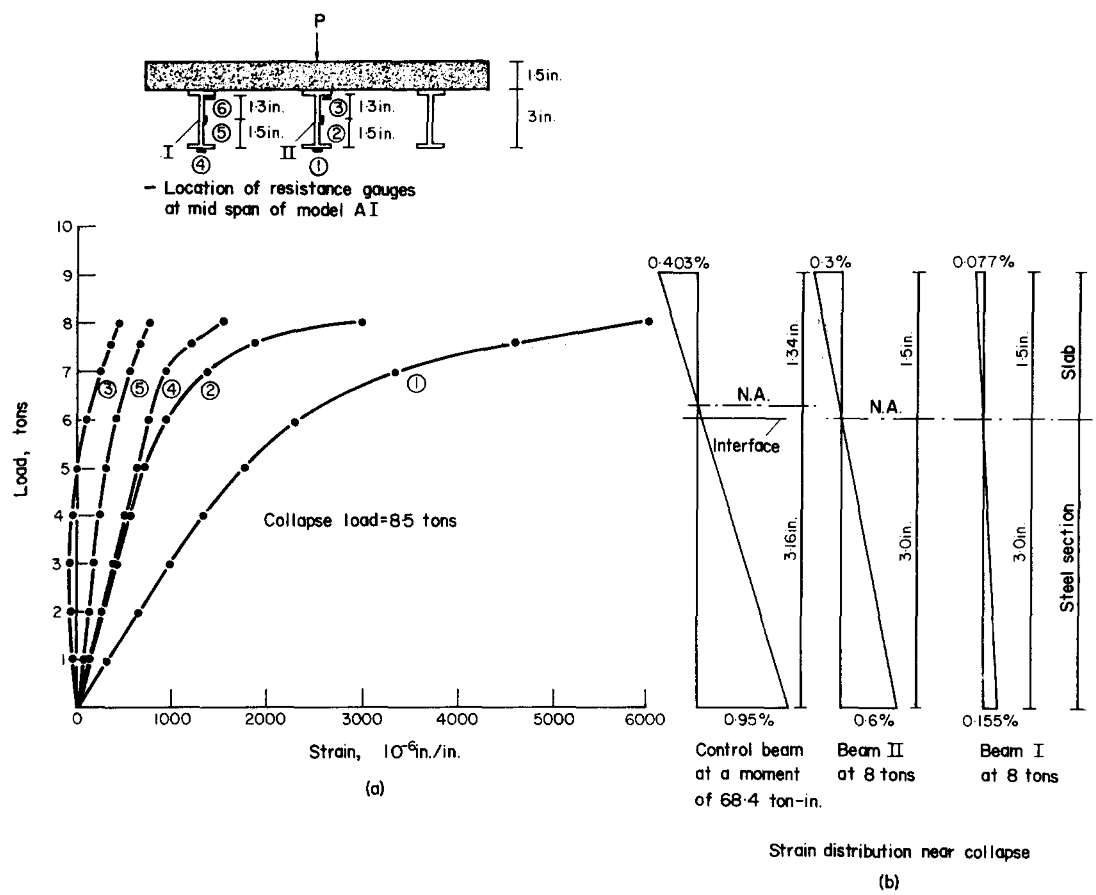

Fig. 8.

In the case of Models A I and A II, yielding did not reach through the entire cross section of the loaded beam, though strain-hardening had commenced in the bottom flange and the deflections there were increasing rapidly. Yielding occurred in the bottom flanges of outer beams but did not penetrate deeper into the steel section. The outer beams were still acting as strong supports to the slab, when failure occurred due to punching of the slab (figure 6).

In the case of Model A III, yielding reached through the entire cross section of the loaded (outer) beam while strain-hardening was taking place in the bottom flange and web. Yielding had penetrated nearly half the depth of the steel section of the central beam. The outer (unloaded) beam was far from the yielding stage and deflected upwards at mid span.

The behaviour of individual beams in B-series was similar to that in A-series, under similar loading but the behaviour of the bridge deck models was, to some extent, different.

In models B I and B II which were comparable to Model A III as regards type of loading, the outer beams (unloaded) were far from the yielding stage and deflected upwards as in Model A III. In model B III, the loading on which is comparable to that on models A I and A II, there is no punching of the slab (figure 16) and the outer beams (unloaded) also failed at ultimate load, which was not the case with the Models A I and A II.

The notable feature in all the models tested was that the outer beams, when loaded, produced relatively larger strains and deflections than the loaded central beams at their corresponding sections at failure. The loaded beams, whether inner or outer, tended to separate from the rest of the bridge deck near ultimate load. The final modes of

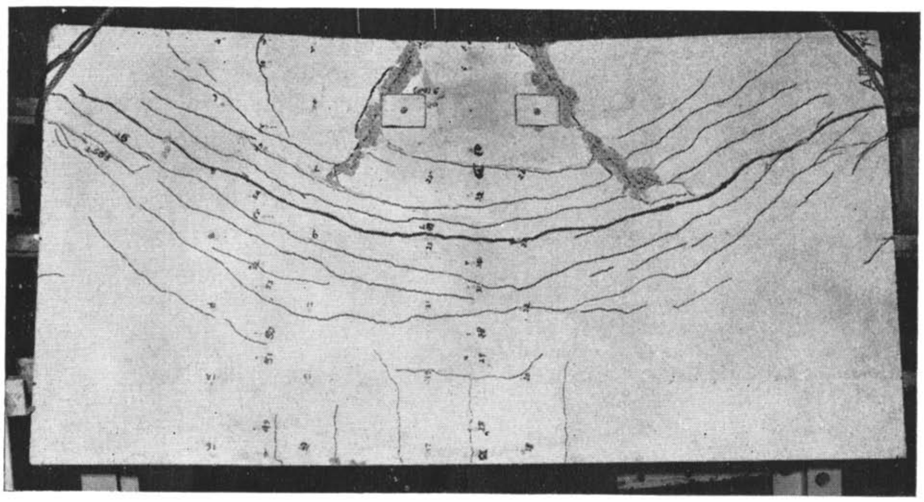

(i) Top

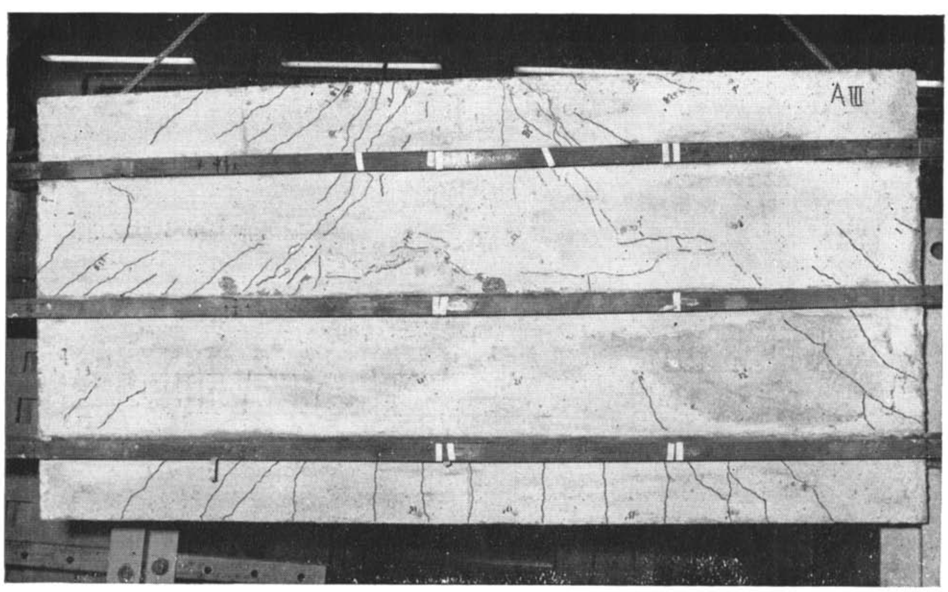

(ii) Bottom

Fig. 9. Crack pattern of Model AIII after failure.

collapse were influenced by the relative strengths of the deck in two orthogonal directions. In all the tests, the loaded beams failed or nearly failed. The beams, two spacings away from the loaded ones, were not greatly affected.

BEHAVIOUR OF MODEL BRIDGES

(*figures* 6–17)

The cracks in the slabs in majority of the tests, were not wide since the reinforcement in the slab consisted of steel with high yield strength (Table 4) and low elongation. There were many small cracks by the side of larger ones. The assumption that full moment of resistance developed along the yield lines was not realised in some tests where the ends of unloaded beams were not anchored down to prevent their lifting up due to eccentricity of the load applied. Only in Model A III, where the ends of the two unloaded beams were firmly anchored down, there was a negative yield line along which the full moment could be assumed to have developed. The positive yield lines were also well formed in this case as seen in figure 9. The ratios of yield load to ultimate load obtained from the test-results varied from 1·77 to 1·89 in models of A-series and from 2·11 to 2·47 in models of B-series. The steel used in beams of A-series had higher strength at first yield than the steel used in beams of B-series.

PUNCHING FAILURE OF SLAB

The load distribution plate 4 in. × 4 in. × $\frac{1}{2}$ in. size punched through the slab in Model A I and A II, where the loading consisted of a single point load at mid span over the central beam. The probable causes for this punching are:

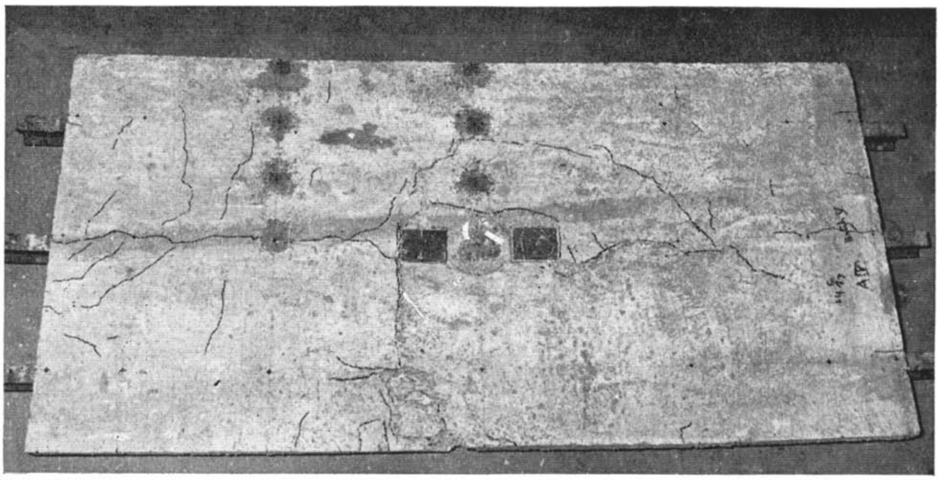

(*i*) *Top*

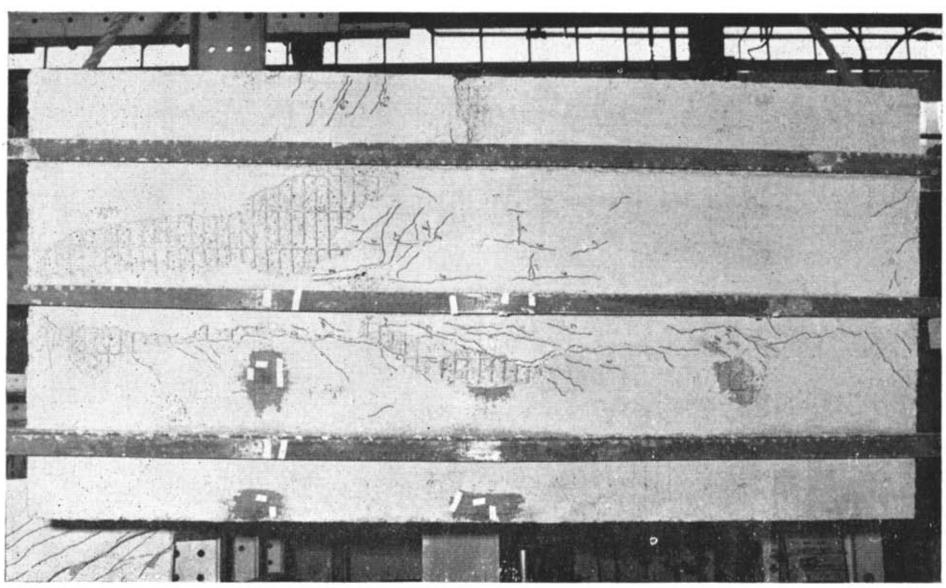

(*ii*) *Bottom*

Fig. 10. *Crack pattern of Model AIV after failure.*

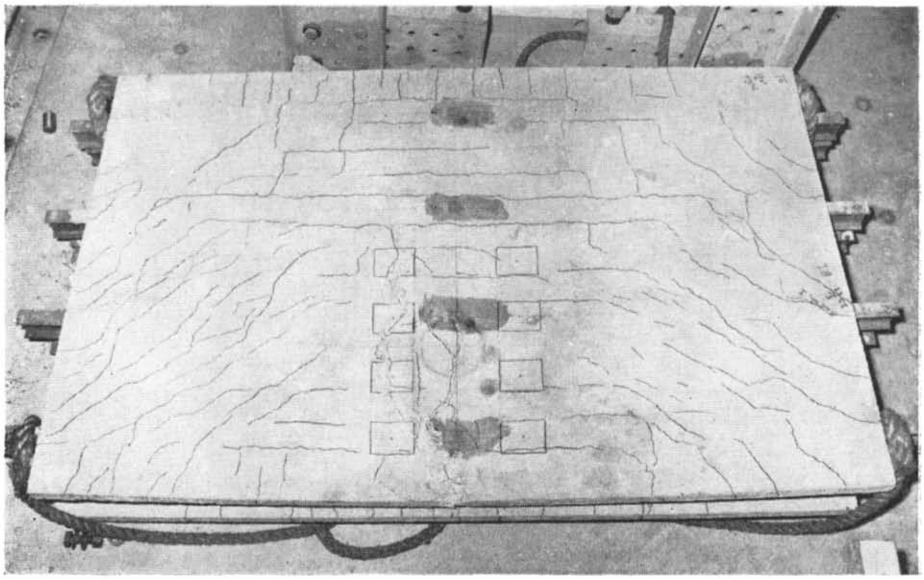

(i) Top

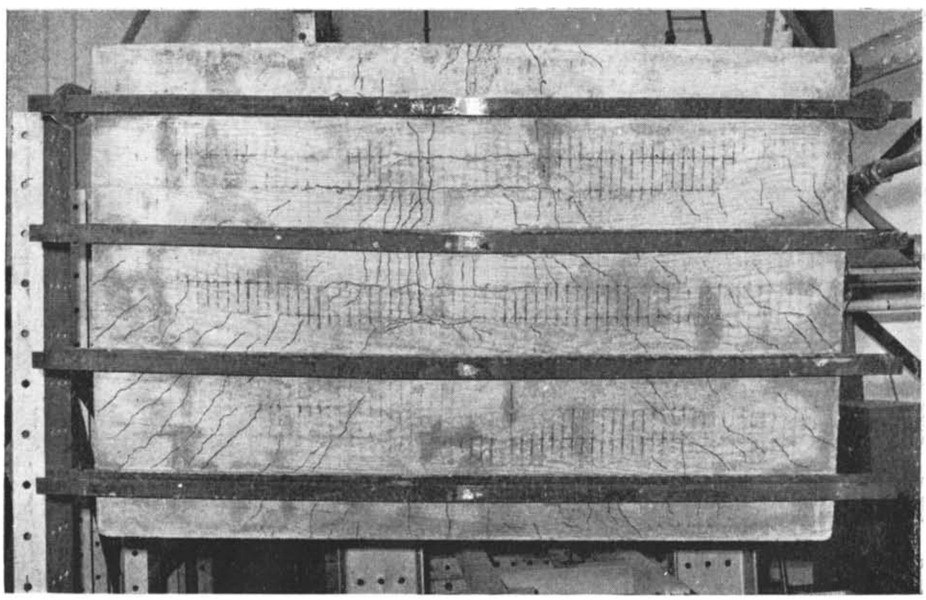

(ii) Bottom

Fig. 11. *Crack pattern of Model BI after failure.*

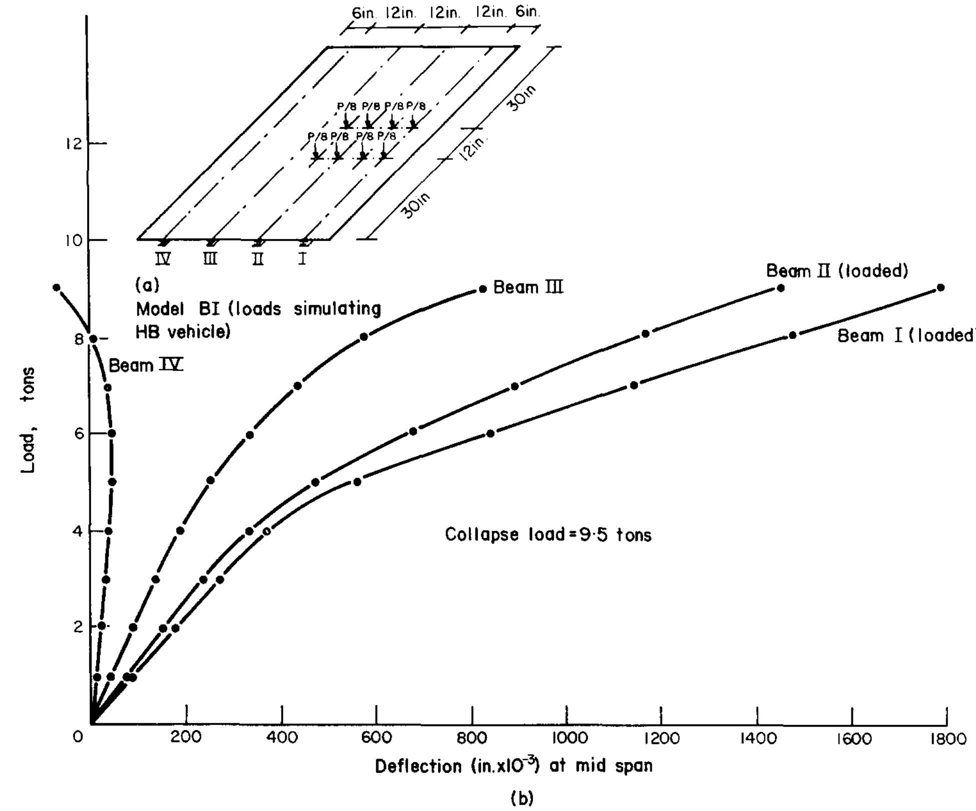
6in. 12in. 12in. 12in. 6in.
P/8 P/8 P/8 P/8
P/8 P/8 P/8 P/8
30in
12in
30in
IV III II I
(a)
Model BI (loads simulating HB vehicle)
Beam III
Beam II (loaded)
Beam I (loaded)
Beam IV
Load, tons
Collapse load = 9·5 tons
0 200 400 600 800 1000 1200 1400 1600 1800
Deflection (in.x10⁻³) at mid span
(b)

Fig. 12.

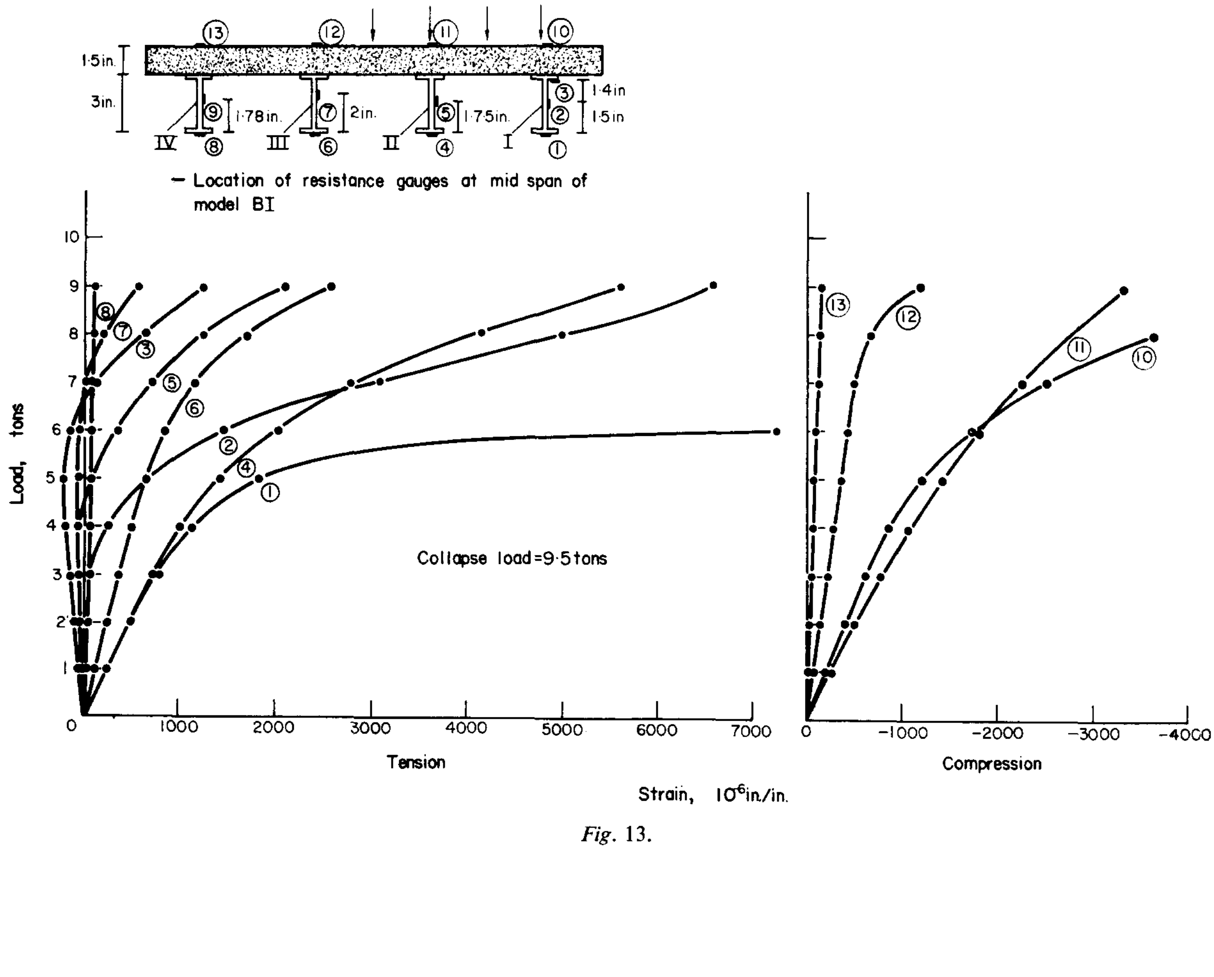
1·5in.
3in.
1·78in.
2in.
1·75in.
1·4in
1·5in
IV III II I
— Location of resistance gauges at mid span of model BI
Load, tons
Collapse load = 9·5 tons
0 1000 2000 3000 4000 5000 6000 7000
Tension
0 −1000 −2000 −3000 −4000
Compression
Strain, 10⁻⁶in./in.

Fig. 13.

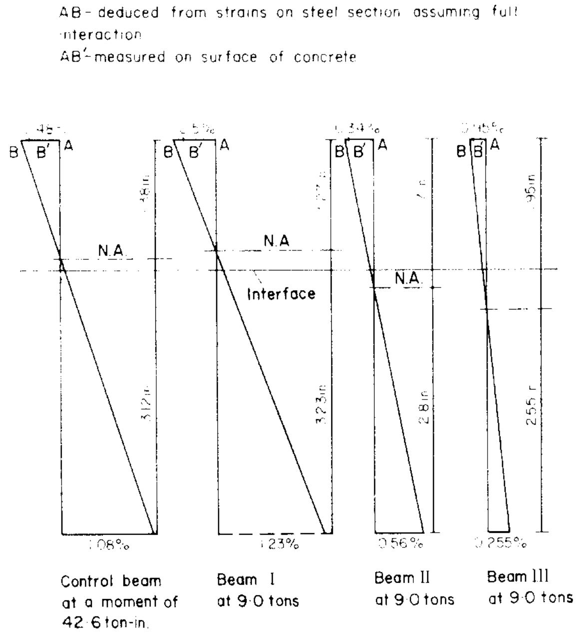

Fig. 14.

(i) inadequate size of distribution plate under the point load,

(ii) stress concentration near the loaded area subjected to high vertical shear

and (iii) vertical separation of the slab from the steel joist.

In the later tests, causes (i) and (ii) were removed by applying two-point loading. There was no punching of slab in Models A IV and B IV, which were subjected to similar loading (figures 10 and 17).

Laboratory tests[10, 11] indicate that, when a single load was placed over a panel, failure occurred as a result of punching shear, i.e. by separation from the slab of a truncated conical section. In Model B I, the loads over the panels were accompanied by loads over the joists and there was no punching (figure 11).

(i) Top

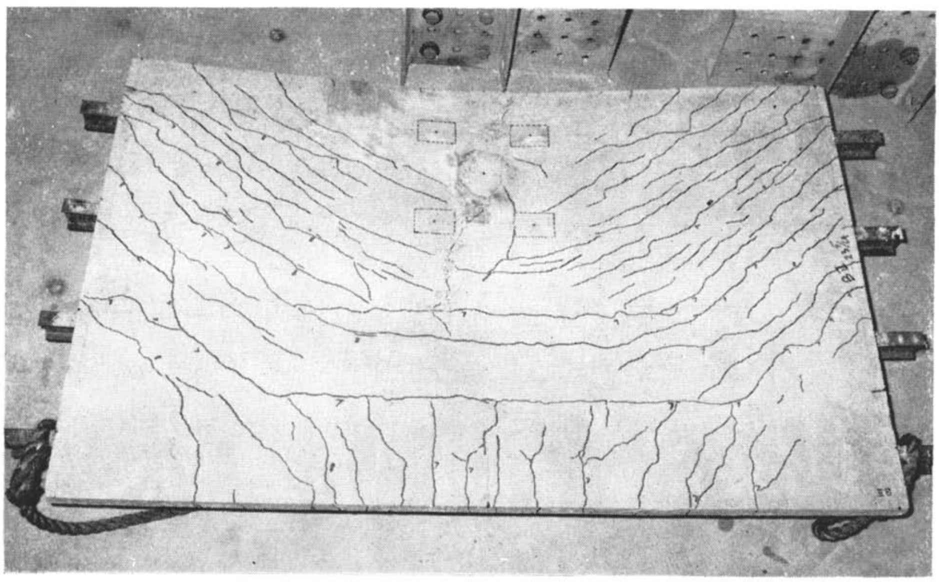

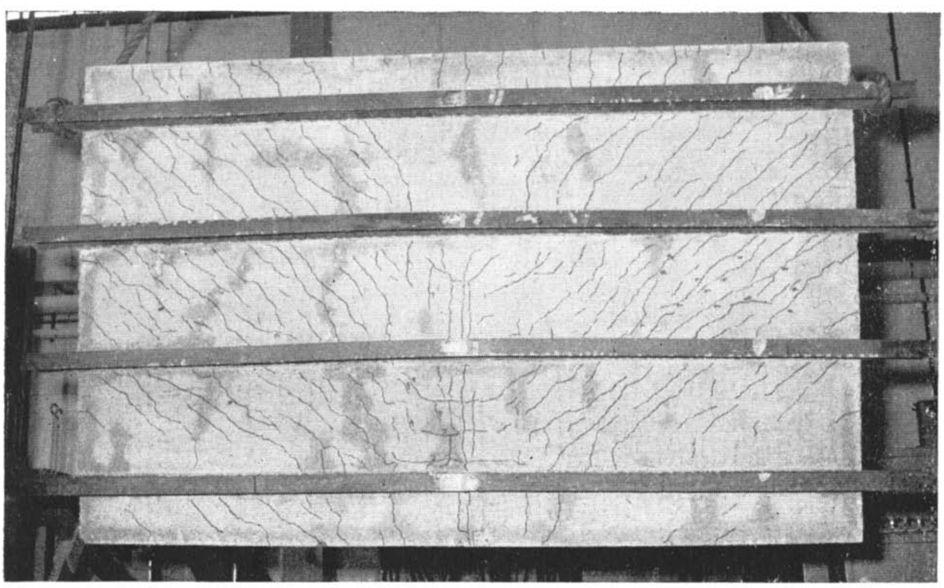

(ii) Bottom

Fig. 15. Crack pattern of Model BII after failure.

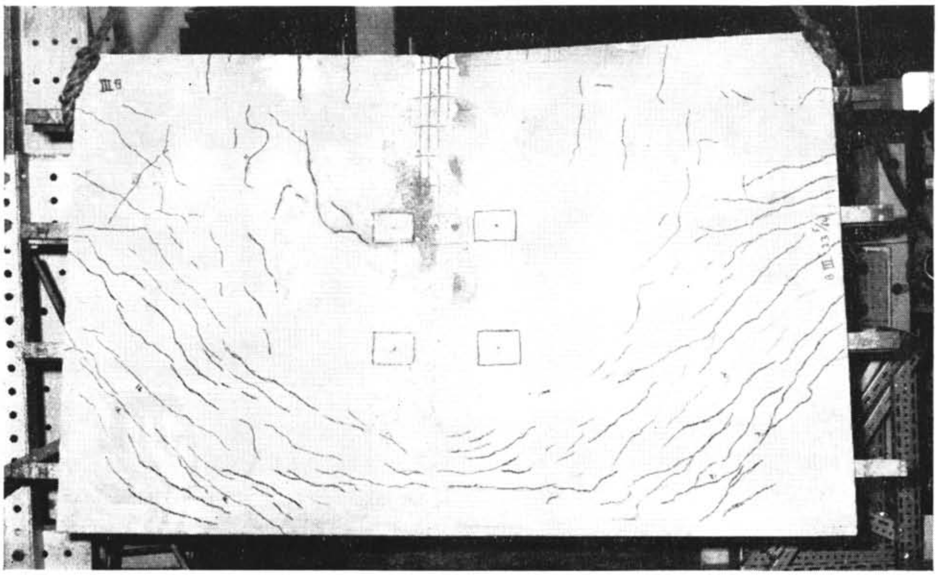

(*i*) *Top*

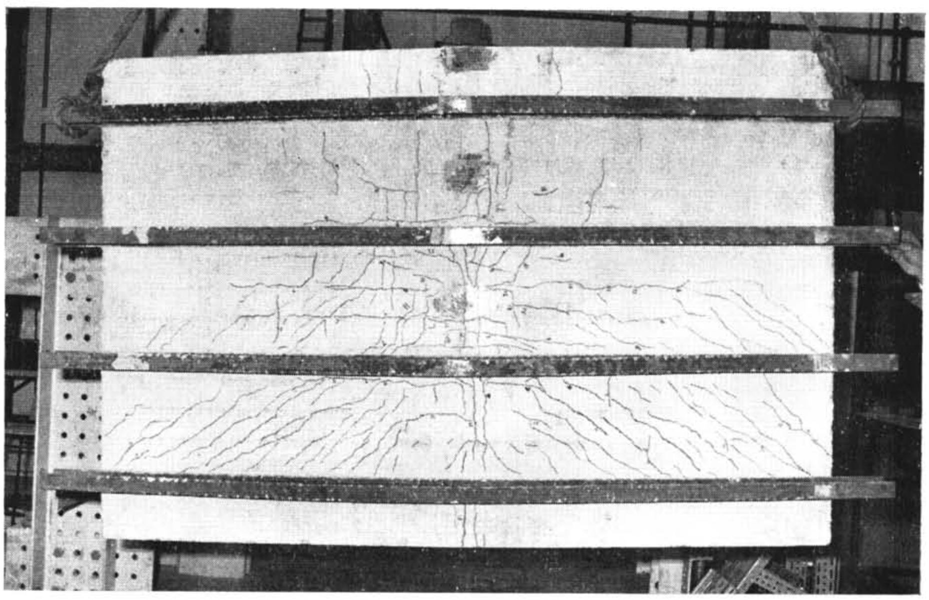

Fig. 16. *Crack pattern after failure of Model BIII.*

(*ii*) *Bottom*

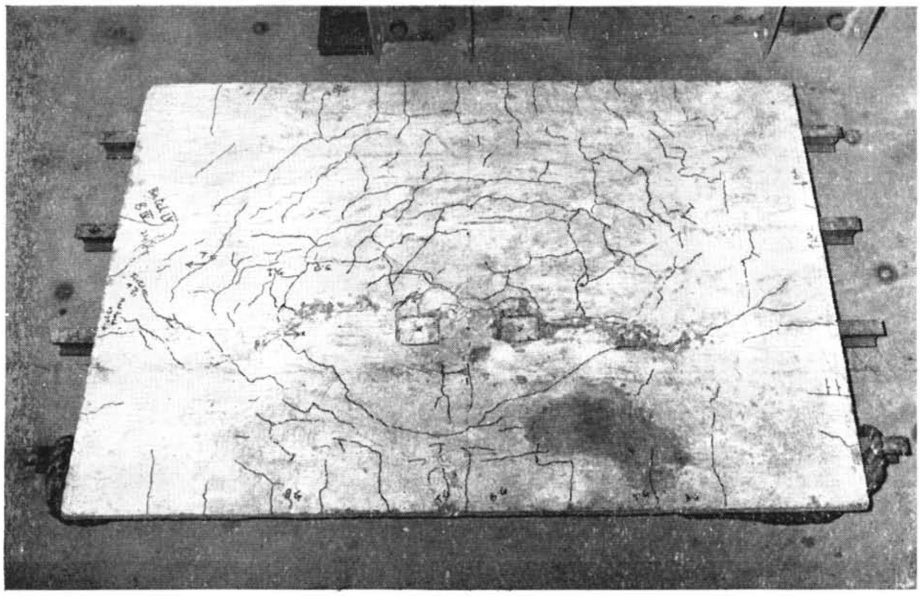

Fig. 17. *Crack pattern at top of Model BIV after failure.*

CONCLUSIONS

(a) The satisfactory measure of agreement between theory and experiment[Table 6] indicates that the approach of the simplified yield-line theory for assessing the ultimate load of a composite beam bridge is adequate for purpose of design. The tendency of the tests to give greater ultimate loads than the theory may be mainly attributed to (i) membrane effect inherent in T-beam action and (ii) strain-hardening of steel, where it occurred.

(b) The experiments described in this paper indicate that it is possible to obtain much useful information on the ultimate load behaviour of bridge decks, using small-scale models. However, a limited programme of tests on full-size bridges would be required to provide conclusive evidence regarding the validity of any theoretical analysis.

(c) The ratios of yield load to ultimate load of model bridges obtained from the tests show that a load factor higher than 2·5 may be necessary, depending on the strength at first yield of the steel used in the beams.

(d) The chances of failure of a bridge deck due to punching of slab are less if the point loads over a panel or panels are accompanied by other point loads over the beams as in a multi-point loading simulating the wheel loads of a HB vehicle.

REFERENCES

1. Composite Construction in structural steel and Concrete. C.P.117 part 2. Beams for bridges. British Standards Institution, London (1967).
2. J. C. Chapman and S. Balakrishnan, Experiments on composite beams, *Struct. Eng*, **42,** Nov. (1964).
3. P. R. Barnard and R. P. Johnson, Ultimate strength of composite beams, *Proc. Inst. Concr. Engrs.*, **32,** Oct. (1965).
4. V. M. Reddy, The ultimate load behaviour of composite steel-concrete bridge deck structures, Ph.D. Thesis, University of Edinburgh (1968).
5. L. L. Jones and R. H. Wood, *Yield-line analysis of slabs* Thames & Hudson; Chatto & Windus (1967).
6. Composite Construction in Structural steel and Concrete. C.P.117 part 1, British Standards Institution, London (1965).
7. I. H. Yuille, Shear lag in stiffened plating. *Trans. Inst. Naval Architects*, **97,** (1955).
8. C. P. Siess, I. M. Viest and N. M. Newmark, Studies of slab and beam highway bridges Part III. Small scale tests of shear connectors and composite T-beams. *Univ. Illinois Enging Exp. Stn Bull.*, No. 396.
9. E. Hognestad, N. W. Hanson and D. McHenry, Concrete stress distribution in ultimate strength design, *J. Am. Concr. Inst.*, **27,** (4), Dec. (1955).
10. F. E. Richart and R. W. Kluge, Tests of reinforced concrete slabs subjected to concentrated loads, *Univ. Illinois Exp. Stn. Bull.*, No. 314, (1939).
11. G. D. Base, *Some tests on punching shear strength of reinforced concrete slabs.* Cement and Concrete Association, London.
12. V. M. Reddy and A. W. Hendry, Ultimate load behaviour of composite steel concrete bridge deck structures, *Indian Concr. J.*, May (1969).

Cet article décrit des essais effectués sur des poutres composites acier/béton de modèle de tablier de pont. Le but des travaux rapportés est d'offrir des données expérimentales pour le développement de méthodes théoriques de prédiction de résistance extrême des tabliers de ce genre de pont, basées sur une analyse du fléchissement linéaire. Des tabliers de pont à simple support avec trois ou quatre éléments longitudinaux furent essayés en diverses conditions de charge.

Dieser Artikel beschreibt Prüfungen an acht Modell-Brückenfahrbahnen aus Stahlträgern und Betonplatten (Verbundkonstruktion). Der Zweck des Arbeitsberichts war, Daten für die Entwicklung einer theoretischen Methode zur Vorraussage der äussersten Stärke von Brückenfahrbahnen dieser Art im Experimentrahmen zu geben, welche auf Bruchlinien-analyse basiert sind. Freiaufliegende Brückenfahrbahnen mit drei und vier Längsträgern wurden unter einer Anzahl von Belastungsverhältnissen geprüft.